Talanta 241 (2022) 123256

Contents lists available at ScienceDirect

Talanta

journal homepage: www.elsevier.com/locate/talanta

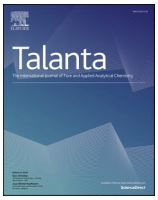

Digital-resolution and highly sensitive detection of multiple exosomal small RNAs by DNA toehold probe-based photonic resonator absorption microscopy

Bin Zhao [a,b], Weijing Wang [b,c], Nantao Li [b,d], Teresa Garcia-Lezana [f], Congnyu Che [b,c], Xiaojing Wang [b], Bojan Losic [f,1], Augusto Villanueva [f], Brian T. Cunningham [a,b,c,d,e,*]

[a] Carl R. Woese Institute for Genomic Biology, University of Illinois at Urbana–Champaign, Urbana, IL, 61801, USA
[b] Nick Holonyak, Jr. Micro and Nanotechnology Laboratory, University of Illinois at Urbana–Champaign, Urbana, IL, 61801, USA
[c] Department of Bioengineering, University of Illinois at Urbana–Champaign, Urbana, IL, 61801, USA
[d] Department of Electrical and Computer Engineering, University of Illinois at Urbana–Champaign, Urbana, IL, 61801, USA
[e] Cancer Center at Illinois, University of Illinois at Urbana-Champaign, Urbana, IL, 61801, USA
[f] Division of Liver Diseases, Division of Hematology / Medical Oncology, Tisch Cancer Institute, Department of Medicine, Icahn School of Medicine at Mount Sinai, New York, NY, 10029, USA

ARTICLE INFO

Keywords:
Photonic resonator absorption microscopy
exosomal small RNAs
DNA toehold probe
active capture + digital counting
cancer diagnostics

ABSTRACT

Small noncoding RNAs (snRNA) have been emerging as promising diagnostic biomarkers for detecting early stage cancer. Currently existing methods for snRNA detection, including northern blot, reverse transcription-polymerase chain reaction, microarrays and RNA-Seq, are limited to time-consuming, low sensitivity, expensive instrumentation or complex analysis of data. Herein, we present a rapid quantitative analysis of multiple liver cancer-associated exosomal snRNA by a nucleic acid toehold probe-based photonic resonator absorption microscopy (PRAM) assay, with digital resolution and high sensitivity. The assay relies on the use of three toehold probe-encoded gold nanoparticles (AuNPs) and addressable photonic crystal (PC) sensing chips. The presence of target snRNA will initiate toehold-mediated strand displacement reactions that trigger the capture of gold particles onto the PC surface, which is subsequently imaged by PRAM for digital counting of detected snRNA molecules. We achieved highly sensitive and selective detection of three snRNA targets in buffer with a 30 min assay protocol, with detection limits of 4.56 fM, 4.68 fM and 0.69 pM. Having confirmed our assay's performance for detection of snRNA targets spiked into exosomal RNA extracts, we demonstrated its capability for quantitative detection of the same targets from patient blood plasma samples. The approach offers a rapid, simple workflow that operates at room temperature with a single step without enzymatic amplification, while the detection instrument can be implemented as a low-cost portable system for point of care environments.

1. Introduction

Small RNA are short, non-coding RNAs that play important roles in regulating gene expression in development and cancer biology [1,2]. There are three main classes of small RNAs, including microRNAs (miRNAs), small interfering RNAs (siRNAs) and piwi-interacting RNAs (piRNAs) [3]. Currently, there are several methods for detecting small RNAs, including reverse transcription-polymerase chain reaction (RT-PCR), northern blot, microarrays and RNA-Seq [4–8]. However, these techniques have several drawbacks that include time-consuming complex workflows, insufficient sensitivity, expensive instrumentation, and complex data analysis [9,10]. Therefore, there are ever-increasing demands to develop rapid, simple and inexpensive approaches for highly sensitive detection of small RNA. In recent years, extracellular vesicles (especially exosomes) have been identified as promising sources for clinically relevant molecular biomarkers for multiple cancers due to their quick and easy accessibility [11,12], and small RNAs encapsulated in exosomes have been emerging as important diagnostic biomarkers for detecting early stage cancers [13]. Rapid and quantitative analysis of multiple exosomal small RNAs still remains

* Corresponding author. Carl R. Woese Institute for Genomic Biology, University of Illinois at Urbana–Champaign, Urbana, IL, 61801, USA.
E-mail address: bcunning@illinois.edu (B.T. Cunningham).
[1] Current affiliation: Guardant Health, Redwood City, CA 94063, USA.

https://doi.org/10.1016/j.talanta.2022.123256
Received 9 November 2021; Received in revised form 16 January 2022; Accepted 20 January 2022
Available online 22 January 2022

challenging.

Small RNA clusters (smRCs) have been identified with important clinical relevance to early hepatocellular carcinoma (HCC) [13]. It is found that three specific smRCs were significantly overexpressed in circulating extracellular vesicles of HCC patients compared to controls at risk or patients with non-HCC malignancies. An independent validation in a phase 2 biomarker study revealed 86% sensitivity and 91% specificity for the detection of early HCC from controls at risk. The 3-smRC signature from plasma capable of detecting early stage HCC directly leads to the prospect of a minimally-invasive, blood-only, operator-independent surveillance biomarker.

Recently, we developed a novel form of metamaterial-enhanced microscopy, named photonic resonator absorption microscopy (PRAM), where the local reflected resonant intensity from a photonic crystal (PC) surface is substantially reduced by the presence of individual gold nanoparticles (AuNPs) [14,15]. The PRAM system enables observation of single particles and digital-resolution counting of detected target molecules. In a typical PRAM image, each black dot represents one single AuNP corresponding to one detected target molecule. Using the PRAM instrument, we demonstrated a toehold DNA–AuNP–based PRAM assay for digital-resolution detection of microRNA [14]. Furthermore, the system has been applied to detect protein biomarkers in serum, including HIV-1 capsid antigen and COVID-19 antibody [16,17].

In this work, we developed a diagnostic platform for rapid quantitative analysis of multiple exosomal small RNAs with digital-resolution and high sensitivity, based on the DNA toehold probe-mediated "Activate Capture + Digital Counting" (AC + DC) PRAM assay. In the AC + DC assay, functionalized AuNPs are activated by target molecules and selectively pulled down to a PC biosensor surface immobilized with capture probes. Utilizing the enhanced absorption of the AuNPs induced by the synergistic plasmonic-photonic coupling [18,19], each captured AuNP on the PC surface is digitally counted with high signal-to-noise ratio, thus enabling single-particle resolution detection. While the AC + DC approach demonstrates attomolar-scale sensitivity for nucleic acid quantification over 5 logs of concentration dynamic range, the response time of the assay is limited by mass transport of activated AuNPs to the PC biosensor surface, which can require 30–120 min to achieve 0.1 fM concentrations [20,21].

The presence of target small RNA will trigger toehold-medicated strand displacement on a AuNP, which "activates" it by exposure of a capture sequence which allows for the AuNP to be selectively captured by a complementary nucleic acid sequence on the PC surface. The captured AuNP is imaged by PRAM and digitally counted for the quantitative analysis. Three HCC-associated small RNAs in the form of smRCs are detected simultaneously by using specific DNA toehold probe-encoded AuNPs and addressable 6-well array chips. This assay offers femtomolar sensitivity and high specificity with a 30-min single step protocol, which is performed at room temperature without target amplification or washing steps. We report herein, for the first time, the successful application of our PRAM-based AC + DC assay for the analysis of small RNAs in clinical samples. Therefore, the method holds great potential for cancer diagnostics in clinical practice.

2. Experimental section

2.1. Preparation of DNA toehold probe-encoded AuNPs

The DNA toehold probe-encoded AuNPs were prepared by annealing Probe DNA-conjugated AuNPs to a stoichiometric amount of Protector DNA. All the DNA and small RNA sequences are listed in Table S1. First, Probe DNA-conjugated AuNPs were prepared by covalently conjugating urchin-shaped AuNPs with thiol-modified Probe DNA with a maleimide gold NanoUrchin conjugation kit (Cytodiagnostics, Burlington, Ontario). Thiol-modified Probe DNA was first reduced with 5 mM of dithiothreitol (Sigma-Aldrich) in 1 × TE buffer (Sigma-Aldrich) at room temperature for 2 h. After 4 times extraction with ethyl acetate (Sigma-Aldrich), the reduced Probe DNA was diluted to 6.4 nM using reaction buffer provided by the kit. The probe was then immediately added to the kit-provided lyophilized 80 nm maleimide gold NanoUrchin, and incubated at room temperature for 1 h with gentle shaking. Probe DNA-conjugated AuNPs were centrifuged at 400 g for 30 min and dispensed with 1 × TE buffer containing 12.5 mM $MgCl_2$ (Sigma-Aldrich) and 0.025% Tween-20 (Sigma-Aldrich). Subsequently, the conjugated AuNPs were annealed to Protector DNA by heating to 80 °C for 2 min and cooling to 18 °C at a rate of 1 °C/min using an Eppendorf 5331 Master Cycler Gradient Thermal Cycler. The as-prepared toehold probe-encoded AuNPs were stored at 4 °C for future use.

2.2. Fabrication and surface functionalization of PC sensing chips

The PC structure used in this work, reported previously [22], is comprised of a low refractive index periodic grating structure that is coated with a higher refractive index material (TiO_2). PCs are fabricated on glass wafers deposited with a 10 nm etch stop layer of Al_2O_3. The periodic grating patterns are constructed by depositing a layer of SiO_2 followed by large area ultraviolet interference lithography performed by Moxtek (Orem, Utah, USA). Finally, a thin layer of TiO_2 (thickness ~100 nm) is deposited on the etched wafers. The resulting PC covers a surface area of 1 × 1.6 cm. The PC is designed to function as a narrowband optical resonator that optimally reflects $\lambda = 625$ nm under water immersion [22].

The PRAM instrument is built upon the body of a bright field microscope (Carl Zeiss Axio Observer Z1) with 20 × or 40 × objective lens as described previously [22]. The optical components consist of an optical fiber-coupled broadband light-emitting diode (LED, Thorlabs M617F1, $600 < \lambda < 650$ nm) source, a polarizing beam splitter (PBS) to collimate and filter the fiber output and a cylindrical lens (f = 200 mm) to focus the polarized light onto the objective back focal plane. As a result, a line-profiled light beam which is polarized perpendicular to the PC grating lines illuminates the PC from below at normal incidence through the microscope objective. The reflected light is then collected by the objective and directed to an imaging spectrometer (Acton Research) where the reflectance spectrum can be obtained by a charge-coupled device camera (Photometrics Cascade, 512 × 512 pixels). By scanning along the PC grating direction, a 2D PRAM image can be obtained by assigning respectively the reflection peak intensity to each pixel within the scanned area.

The PC surface was first silanized by coating a layer of (3-Glycidyloxypropyl) trimethoxysilane (GPTMS, Sigma Aldrich) in an 80 °C vacuum for 6 h. After post-washing to remove the redundant GPTMS, a PDMS gasket with six circular openings (diameter = 3 mm) was placed onto the PC surface to form 6-well array chips. The PC was then immobilized with Capture probe by adding 10 μL of 10 μM Capture Probe into each well and incubating overnight at room temperature. After washing with 1 × TE, SuperBlock™ (PBS) Blocking Buffer (ThermoFisher Scientific) was added into each well and incubated at room temperature for 30 min to minimize the non-specific binding of AuNPs during the assay.

2.3. Digital detection of small RNAs

Typically, a 2 μL volume of small RNA-containing sample was mixed with each type of DNA toehold probe-encoded AuNPs specific to each target small RNA in a tube. After mixing well, the mixture was immediately applied to its corresponding compartment of 6-well array chips to detect its corresponding target small RNA. For instance, 2 μL of test sample (exosomal extract with spiked small RNAs, or total exsomal RNA isolated from patient/healthy samples) was mixed with toehold probe-135,709 encoded AuNPs in 1 × TE buffer containing 12.5 mM $MgCl_2$ (Sigma-Aldrich) and 0.025% Tween-20 and the well-mixed solution was added to channel 135,709 on a PC sensing chip. PRAM imaging was

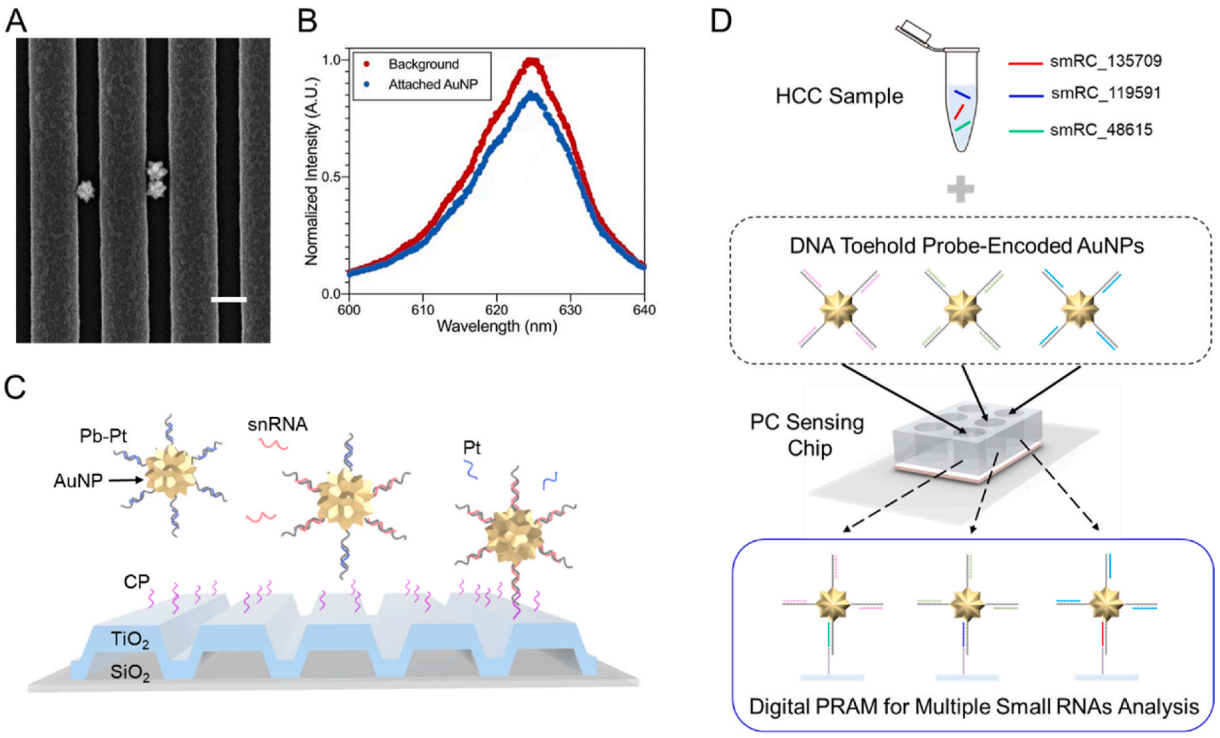

Fig. 1. DNA toehold probe-based digital PRAM assay. (**A**) SEM image of urchin-like AuNPs on PC surface. Scale bar: 200 nm. (**B**) Reflection spectra of PC with attached AuNP (blue) and without AuNP attachment (Background, gray). (**C**) 3D scheme illustrating the principle of DNA toehold probe-based digital PRAM assay for smRNA detection. The target smRNA (red line) through toehold probe –mediated strand displacement reaction resulting in the active capture of AuNPs onto PC surface. (**D**) Toehold probe-encoded AuNPs-based analysis on addressable 6-well array sensing PC chips for the detection of three small RNAs, smRC_135,709, smRC_11,959 and smRC_48,615. Pb: Probe DNA, Pt: Protector DNA, Pb–Pt: Toehold probe, snRNA: Target small non-coding RNA, CP: Capture DNA, PC: Photonic crystal, HCC: Hepatocellular carcinoma patient samples. (For interpretation of the references to colour in this figure legend, the reader is referred to the Web version of this article.)

performed after 30 min of incubation with the test sample in the well, by scanning a 150 × 150 μm^2 PC surface area in each well. As described in prior publications [14,16], the raw PRAM images are first filtered in the Fourier plane to remove nonuniform background caused by line scanning. Next, maximally stable extremal regions (MSER) is used to detect the blob shapes presented in the images. Each detected region is then respectively gauged with regards to its orientation, total size, eccentricity and averaged signal intensity. Finally, the detected shapes satisfying the selection criteria are enumerated.

2.4. Human samples

Blood samples were collected from patients with hepatocellular carcinoma diagnosed using the AASLD criteria [23]. Patients consented for the use of samples for research and the study was approved by the IRB at the Icahn School of Medicine at Mount Sinai (HS-15–00540).

3. Results and discussion

3.1. Design of DNA toehold probe-based digital PRAM assay

Fig. 1 illustrates the working principle of the DNA toehold probe-mediated digital PRAM assay for the detection of multiple small RNAs. Upon the attachment of single AuNPs on PC surface (Fig. 1A), the synergistic plasmonic-photonic coupling between AuNP and PC occurs when the local surface plasmon resonance (LSPR) wavelength of AuNP matches the PC resonant reflection wavelength. As a result, the local reflected resonant intensity from the PC is substantially reduced by the presence of individual AuNPs (Fig. 1B), enabling the observation of single particles by PRAM. Fig. 1C schematically illustrates the design of the toehold probe-based AC + DC PRAM assay for small RNA detection. A DNA toehold probe composed of probe and protector is first conjugated to the urchin-shaped AuNPs. The presence of target small RNA will trigger the strand displacement reaction by binding the probe toehold and displacing the protector, resulting in the exposure of an additional probe sequence. This additional probe sequence will further hybridize with a capture probe pre-immobilized on PC, along with the activated capture of AuNPs onto the PC surface. Then PRAM instrument is subsequently used for imaging individual captured AuNPs, allowing for digital counting for quantitative analysis. The design of addressable 6-well array chips for the detection of three types of small RNAs is schematically illustrated in Fig. 1D. Three types of DNA toehold probe-encoded AuNPs were prepared, which are specific to three target small RNA (named smRC_135,709, smRC_119,591 and smRC_48,615), respectively. These small RNAs have been identified by RNA-seq and clinical studies to correlate with the presence of early stage liver cancer [13]. For each target small RNA, a specific DNA toehold probe was rationally designed by tuning the reaction free energy (ΔG_{rxn}) for the target to zero with additional equivalents of protector (Table S2) [14, 24]; therefore, each toehold probe-modified AuNPs could detect its corresponding small RNA.

In this work, exosomal extracts isolated from HCC patient samples were tested, which contain all three target small RNAs associated with liver cancer [13]. Also, we tested samples from healthy individuals as negative controls. Each of the HCC patient samples or the control samples was mixed with each toehold probe-encoded AuNPs separately. Each mixture was then immediately applied to one of the addressable 6-well array PC sensing chips with capture probe-coated PC comprising the entire bottom surface.

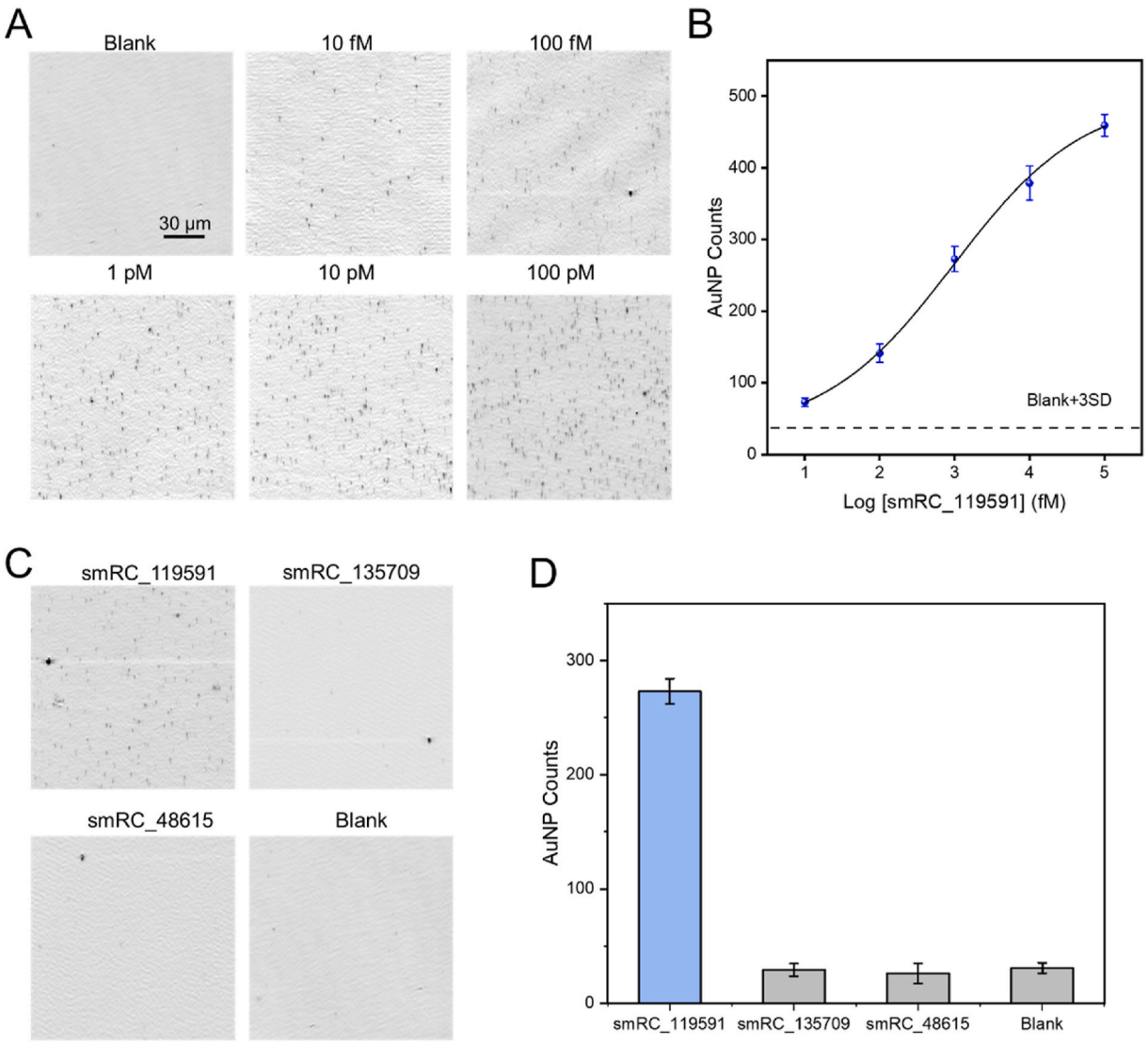

Fig. 2. Sensitive and selective detection of smRC_119,591 by toehold probe-based digital PRAM assay. (**A**) Representative PRAM images for different concentrations of smRC_119,591. Blank represents the negative control performed with no smRC_119,591 in the test sample. (**B**) Particle quantification as a function of smRC_119,591 concentration at 30 min. The dashed horizontal line indicates the threshold equal to blank signal +3 standard deviations (blank + 3SD). (**C**) PRAM images for smRC_119,591, control small RNAs (smRC_135,709 and smRC_48,615) and blank control. The concentration of smRC_119,591, smRC_135,709 and smRC_48,615 is 1 pM. (**D**) Quantification of particle count for comparison of smRC_119,591 and control experiments. The error bars represent the standard deviation of three independent assays.

3.2. Sensitivity and selectivity for small RNA detection

As a proof-of-concept demonstration, we first investigated the performance of the toehold probe-based digital PRAM assay for the detection of synthetic small RNA spiked into buffer. Fig. 2 depicts the sensitivity and selectivity of the method for smRC_119,591. A series of samples containing different concentrations of smRC_119,591 was measured using toehold probe-119,591 -encoded AuNPs by PRAM. As shown in Fig. 2A, the count of particles gradually increased with increased concentration of smRC_119,591 from 0 to 100 pM. The dose-response plot for the for smRC_119,591 assay showed a detection range of 10 fM – 100 pM and the calculated limit of detection (LOD) was 0.25 fM (Fig. 2B). It is noteworthy that the assay is capable of discriminating differences in concentration over the 10 fM – 100 pM concentration range but only a roughly 6-fold difference in AuNP counts (100 pM: 459 ± 18; 10 fM: 73 ± 7) was observed. This is presumably due to the equilibria of binding of activated AuNPs onto PC surface.

We next evaluated the selectivity of the method against other small RNA targets. Two small RNAs, smRC_135,709 and smRC_48,615, were selected as controls. As depicted in Fig. 2C, both control small RNAs (1 pM) show a small number of particles (smRC_135,709: 29 ± 6, smRC_48,615: 26 ± 9) and no significant difference to the blank control (30 ± 5) after 30 min. In contrast, the target small RNA, smRC_119,591, at the same concentration results in an elevated number of particles (273 ± 21) bound to the PC through toehold probe-mediated active capture of AuNPs, which is 9 times higher than that of controls. The results demonstrate our toehold probe-based digital PRAM assay has good specificity towards target smRC_119,591.

Similarly, we demonstrated the capability of the method for sensitive and selective detection of two additional small RNAs, smRC_135,709 and smRC_48,615. As shown in Fig. S1, a dose response was achieved in the concentration range from 10 fM to 100 pM for smRC_135,709 detection. The LOD for smRC_135,709 was calculated to be 3.8 fM. For the detection of smRC_48,615, the assay demonstrated a detection range from 1 pM to 1 nM, and the calculated LOD was 0.36 pM (Fig. S2). We hypothesize that the relative low sensitivity is due to the potential for

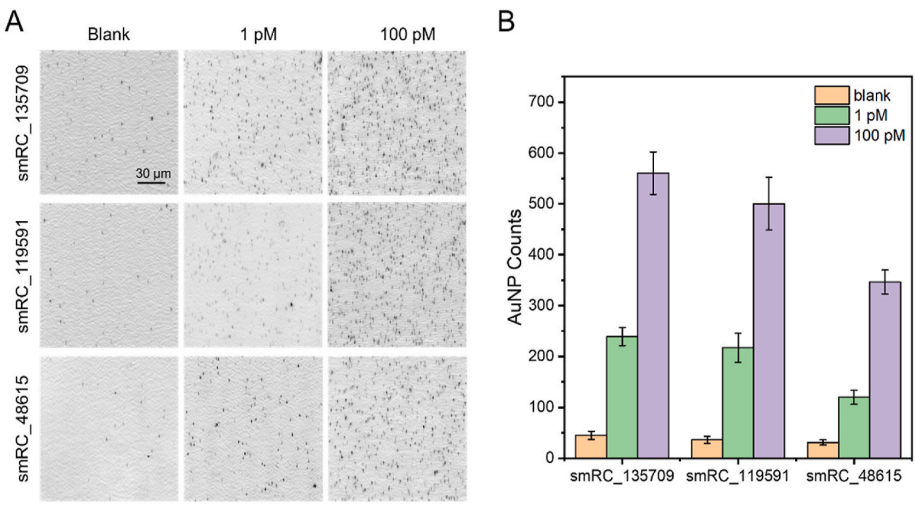

Fig. 3. Digital detection of spiked small RNAs in exosomal extracts. (**A**) Representative PRAM images for analysis of exosomal samples spiked with 100 pM and 1pM of each small RNA at 30 min. Blank represents the negative control with no small RNAs spiked in the test sample. (**B**) Quantitative analysis of particle counts for variable concentration of small RNA-spiked exosomal extract samples at 30 min. The error bars represent the standard deviation of three independent assays.

smRC_48,615 to form a secondary structure (Fig. S3). In both cases, the selectivity test showed that only a small number of particles were observed for control small RNAs, indicating good specificity of the assay towards the target.

3.3. Digital detection of small RNA spiked in exosomal RNA extracts

We next evaluated the performance of the method for the detection of three spiked small RNAs in exosomal RNA extracts. The exosomal RNA extracts were isolated from blood plasma of healthy people and prepared with RNase free water. Given that our method offers a detection range of 1 pM–100 pM for all three small RNAs, 100 pM and 1pM were selected as the representatives of high and low level of spiked small RNAs in exosomal RNA extracts for the analysis.

As shown in Fig. 3, when the concentration of each spiked small RNA is 100 pM, a large number of nanoparticles were observed by PRAM for each spiked small RNA with its corresponding toehold probe-encoded AuNPs. The digitally counted numbers of particles for smRC_135,709, smRC_119,591 and smRC_48,615 are 561 ± 42, 500 ± 52 and 347 ± 24, respectively. For each small RNA at 1pM, all show a moderate number of bound AuNPs (smRC_135,709: 239 ± 18, smRC_119,591: 217 ± 29, and smRC_48,615: 120 ± 14). In contrast, blank controls performed with no small RNAs spiked in the test samples demonstrated low particle counts. It is noteworthy that the quantitative results for the analysis of spiked small RNA in exosomal extracts are in good agreement with experimental results performed in buffer, indicating the standard curves we established can be directly used for the quantification of small RNAs in exosomal extract samples.

3.4. Digital detection of three small RNAs in clinical samples

Having demonstrated AC + DC detection of small RNAs spiked in exosomal extracts, we further challenged the method with clinical patient samples. Total exosomal RNAs containing liver cancer-associated small RNAs were isolated from the blood plasma of four patients, which have been validated with RT-PCR/RNA-Seq. With our method, detectable signals were clearly observed for each type of small RNA in all clinical samples, while the healthy control only show negligible background signals (Fig. 4A). The range of AuNPs counts is 162 ± 17 to 315 ± 32, 162 ± 18 to 239 ± 26 and 66 ± 7 to 121 ± 12, for smRC_135,709, smRC_119,591 and smRC_48,615, respectively (Fig. S4). By contrast, the AuNP counts for healthy control samples ranged between 29 ± 3 to 56 ± 5, which are similar to or below the threshold equal to blank signal +3 standard deviations (blank + 3SD).

Based on the calibration curves we established previously, we estimated the concentration of each small RNA in each HCC patient sample. The concentration of smRC_119,591, smRC_135,709 and smRC_48,615 varied from 4.2 ± 0.8 to 16.3 ± 3.7 pM, 1.2 ± 0.3 to 13.4 ± 3.0 pM and 3.7 ± 0.5 to 16.0 ± 2.5 pM pM. As shown in Fig. 4B–D, PRAM results are in good agreement with RT-PCR results. All the data determined by PRAM and RT-PCR are well correlated, except one for smRC_135,709 (13.4 ± 3.0 pM vs 6.5 pM). Interestingly, we also performed linear regression of dose response of each small RNA for quantitative analysis (Fig. S5). Similarly, a good correlation between PRAM and RT-PCR results was achieved for smRC_119,591 and smRC_48,615 respectively, due to their good linear dose response in the detection range. For smRC_135,709, the agreement is relatively poor because of the lack of linear dose response in the whole detection range. Taken together, the results suggest that our DNA toehold probe-based digital PRAM assay have satisfactory sensitivity and high selectivity for multiple small RNAs analysis in clinical specimens.

4. Conclusions

In summary, we presented a DNA toehold probe-based PRAM digital assay for rapid and quantitative analysis of multiple exosomal small RNAs. The combination of three toehold probe-encoded AuNPs and addressable well array chips enables simultaneous detection of three liver cancer-associated small RNAs, based on the principle of AC + DC by PRAM. Highly sensitive and selective detection of each small RNA was achieved in buffer at 30 min. The method shows satisfactory performance for the analysis of small RNAs in exosomal RNA extracts. Furthermore, we demonstrated its capability for multiple small RNAs analysis in clinical samples. To the best of our knowledge, this work presents the first utilization of PRAM-based AC + DC assay on clinical sample analysis.

Due to its low cost and simplicity, this method is expected to be commercialized by integrating a portable PRAM instrument for point-of-care (POC) testing. Recently, we have reported the design, implementation, and characterization of a portable version of PRAM and demonstrated its versatility for digital-resolution detection of miRNA with 160 aM detection limits in a 30-min assay [21]. The simple, room temperature, single step workflow combined with a compact and portable PRAM instrument will provide precise, highly sensitive, and quantitative measurements for rapid POC diagnostics and therefore significantly improve the diagnostic accuracy in clinical practices [25].

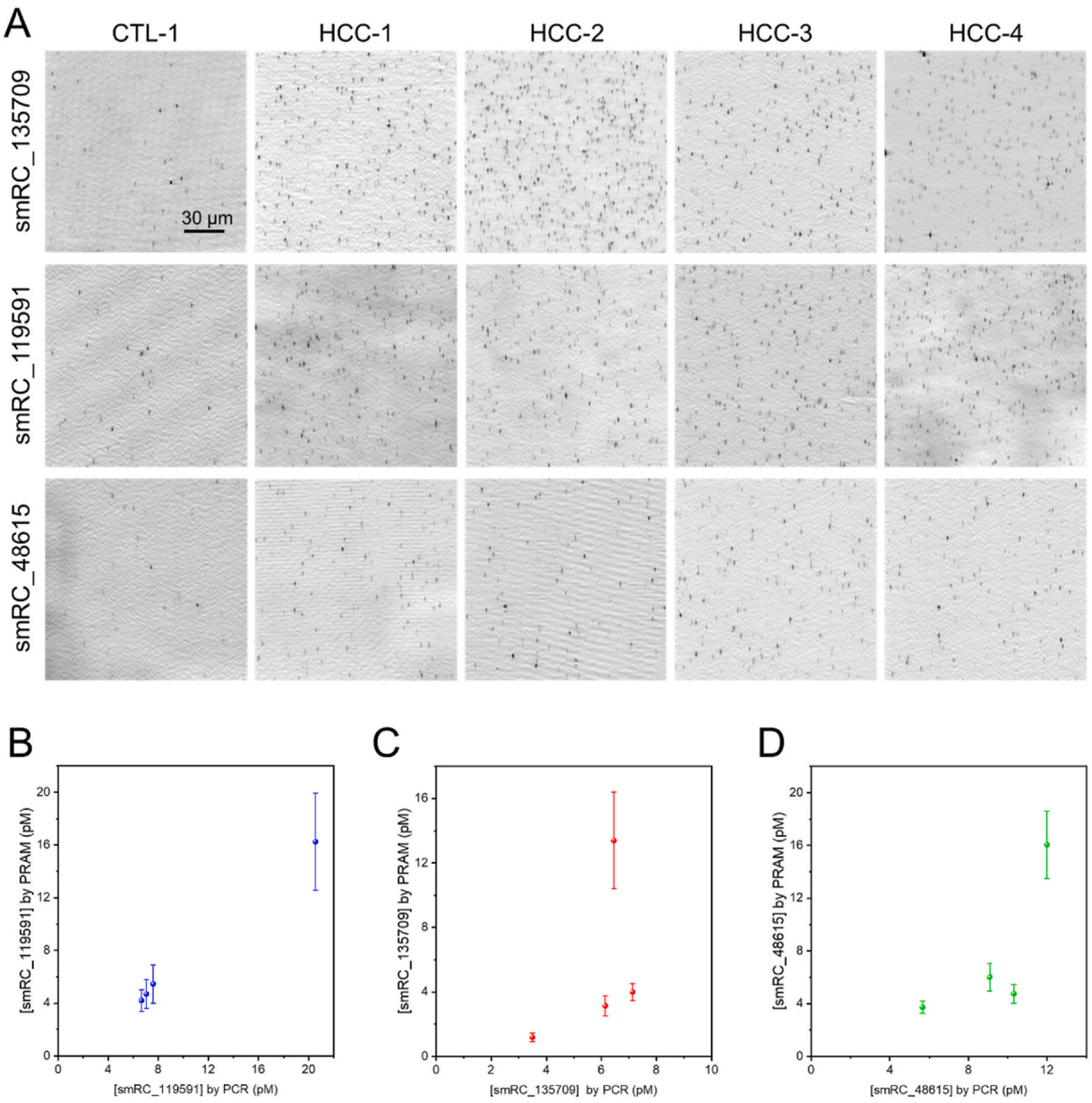

Fig. 4. Analysis of small RNAs in clinical samples. (**A**) Representative PRAM images of healthy (control, CTL) and Hepatocellular carcinoma (HCC) patient samples with toehold probe-based digital PRAM assay at 30 min. (**B-D**) Correlation of small RNA concentration in HCC patient samples determined by PRAM and PCR assay. The error bars represent the standard deviation of three independent assays.

Furthermore, the rational design of the digital sensing platform has potential for the development of universal tools for high-throughput clinical diagnostics.

Credit author statement

Bin Zhao: Methodology, Investigation, Data curation, Validation, Formal analysis, Writing – original draft, Writing – review & editing. **Weijing Wang**: Investigation, Data curation, Validation, Formal analysis, Writing – original draft. **Nantao Li**: Investigation, Data curation, Validation, Formal analysis, Writing – original draft. **Teresa Garcia-Lezana**: Data curation, Validation, Formal analysis, Resources. **Congnyu Che**: Validation, Formal analysis, Writing – original draft. **Xiaojing Wang**: Validation, Formal analysis. **Bojan Losic**: Validation, Resources. **Augusto Villanueva**: Data curation, Validation, Formal analysis, Resources, Writing – review & editing. **Brian T. Cunningham**: Conceptualization, Project administration, Funding acquisition, Writing – review & editing, Supervision.

Declaration of competing interest

The authors declare the following financial interests/personal relationships which may be considered as potential competing interests: AV has received consulting fees from Boehringer Ingelheim, FirstWorld, Natera, Cambridge Healthcare Research and Genentech; advisory board fees from BMS, Gilead and NGM Pharmaceuticals; and research support from Eisai.

Acknowledgements

This work is supported by the National Institutes of Health (NIH) R21 AI130562 (to B.T.C.) and R01 AI20683 (to B.T.C). B. Z. is supported by a Carl R. Woese Institute for Genomic Biology (IGB) fellowship in the Center for Genomic Diagnostics. The authors gratefully acknowledge the

members of the Nanosensors Group (NSG) and staff in the Nick Holonyak Jr. Micro and Nanotechnology Laboratory for their support.

Appendix A. Supplementary data

Supplementary data to this article can be found online at https://doi.org/10.1016/j.talanta.2022.123256.

References

[1] G. Stefani, F.J. Slack, Small non-coding RNAs in animal development, Nat. Rev. Mol. Cell Biol. 9 (2008) 219–230.
[2] Y. Shimoni, G. Friedlander, G. Hetzroni, G. Niv, S. Altuvia, O. Biham, H. Margalit, Regulation of gene expression by small non-coding RNAs: a quantitative view, Mol. Syst. Biol. 3 (2007) 138.
[3] C. Zhang, Novel functions for small RNA molecules, Curr. Opin. Mol. Therapeut. 11 (2009) 641–651.
[4] E. Varkonyi-Gasic, R.P. Hellens, qRT-PCR of Small RNAs, in: I. Kovalchuk, F. J. Zemp (Eds.), Plant Epigenetics: Methods and Protocols, Humana Press, Totowa, NJ, 2010, pp. 109–122.
[5] E. Varkonyi-Gasic, R. Wu, M. Wood, E.F. Walton, R.P. Hellens, Protocol: a highly sensitive RT-PCR method for detection and quantification of microRNAs, Plant Methods 3 (2007) 12.
[6] M.O. Urbanek, A.U. Nawrocka, W.J. Krzyzosiak, Small RNA detection by in situ hybridization methods, Int. J. Mol. Sci. 16 (2015) 13259–13286.
[7] S.W. Kim, Z. Li, P.S. Moore, A.P. Monaghan, Y. Chang, M. Nichols, B. John, A sensitive non-radioactive northern blot method to detect small RNAs, Nucleic Acids Res. 38 (2010) e98-e98.
[8] L.C. Pantaleão, S.E. Ozanne, Small RNA sequencing: a technique for miRNA profiling, in: P.C. Guest (Ed.), Investigations of Early Nutrition Effects on Long-Term Health: Methods and Applications, Springer New York, New York, NY, 2018, pp. 321–330.
[9] J. Koshiol, E. Wang, Y. Zhao, F. Marincola, M.T. Landi, Strengths and limitations of laboratory procedures for microRNA detection, Cancer Epidemiol. Biomarkers Prev. 19 (2010) 907–911.
[10] J. Ye, M. Xu, X. Tian, S. Cai, S. Zeng, Research advances in the detection of miRNA, J. Pharm. Anal. 9 (2019) 217–226.
[11] A. Becker, B.K. Thakur, J.M. Weiss, H.S. Kim, H. Peinado, D. Lyden, Extracellular vesicles in cancer: cell-to-cell mediators of metastasis, Cancer Cell 30 (2016) 836–848.
[12] S.A. Bellingham, B.M. Coleman, A.F. Hill, Small RNA deep sequencing reveals a distinct miRNA signature released in exosomes from prion-infected neuronal cells, Nucleic Acids Res. 40 (2012) 10937–10949.
[13] J. von Felden, T. Garcia-Lezana, N. Dogra, E. Gonzalez-Kozlova, M.E. Ahsen, A. Craig, S. Gifford, B. Wunsch, J.T. Smith, S. Kim, J.E.L. Diaz, X. Chen, I. Labgaa, P. Haber, R. Olsen, D. Han, P. Restrepo, D. D'Avola, G. Hernandez-Meza, K. Allette, R. Sebra, B. Saberi, P. Tabrizian, A. Asgharpour, D. Dieterich, J.M. Llovet, C. Cordon-Cardo, A. Tewari, M. Schwartz, G. Stolovitzky, B. Losic, A. Villanueva, Unannotated small RNA clusters associated with circulating extracellular vesicles detect early stage liver cancer, Gut (2021) gutjnl-2021-325036.
[14] T.D. Canady, N. Li, L.D. Smith, Y. Lu, M. Kohli, A.M. Smith, B.T. Cunningham, Digital-resolution detection of microRNA with single-base selectivity by photonic resonator absorption microscopy, Proc. Natl. Acad. Sci. U.S.A. 116 (2019) 19362.
[15] Q. Huang, N. Li, H. Zhang, C. Che, F. Sun, Y. Xiong, T.D. Canady, B.T. Cunningham, Digital resolution biomolecular sensing for diagnostics and life science research, Lab on a Chip 17 (2020) 2816–2840.
[16] C. Che, N. Li, K.D. Long, M.Á. Aguirre, T.D. Canady, Q. Huang, U. Demirci, B. T. Cunningham, Activate capture and digital counting (AC + DC) assay for protein biomarker detection integrated with a self-powered microfluidic cartridge, Lab Chip 19 (2019) 3943–3953.
[17] B. Zhao, C. Che, W. Wang, N. Li, B.T. Cunningham, Single-step, wash-free digital immunoassay for rapid quantitative analysis of serological antibody against SARS-CoV-2 by photonic resonator absorption microscopy, Talanta 225 (2021) 122004.
[18] J.N. Liu, Q. Huang, K.K. Liu, S. Singamaneni, B.T. Cunningham, Nanoantenna-microcavity hybrids with highly cooperative plasmonic-photonic coupling, Nano Lett. 17 (2017) 7569–7577.
[19] Q. Huang, B.T. Cunningham, Microcavity-mediated spectrally tunable amplification of absorption in plasmonic nanoantennas, Nano Lett. 19 (2019) 5297–5303.
[20] T.D. Canady, N. Li, L.D. Smith, Y. Lu, M. Kohli, A.M. Smith, B.T. Cunningham, Digital-resolution detection of microRNA with single-base selectivity by photonic resonator absorption microscopy, Proc. Natl. Acad. Sci. U.S.A. 116 (2019) 19362–19367.
[21] S. Ghosh, N. Li, Y. Xiong, Y.-G. Ju, M.P. Rathslag, E.G. Onal, E. Falkiewicz, M. Kohli, B.T. Cunningham, A compact photonic resonator absorption microscope for point of care digital resolution nucleic acid molecular diagnostics, Biomed. Opt Express 12 (2021) 4637–4650.
[22] Y. Zhuo, H. Hu, W. Chen, M. Lu, L. Tian, H. Yu, K.D. Long, E. Chow, W.P. King, S. Singamaneni, B.T. Cunningham, Single nanoparticle detection using photonic crystal enhanced microscopy, Analyst 139 (2014) 1007–1015.
[23] J.A. Marrero, L.M. Kulik, C.B. Sirlin, A.X. Zhu, R.S. Finn, M.M. Abecassis, L. R. Roberts, J.K. Heimbach, Diagnosis, staging, and management of hepatocellular carcinoma: 2018 practice guidance by the American association for the study of liver, Diseases 68 (2018) 723–750.
[24] L.R. Wu, J.S. Wang, J.Z. Fang, E.R. Evans, A. Pinto, I. Pekker, R. Boykin, C. Ngouenet, P.J. Webster, J. Beechem, D.Y. Zhang, Continuously tunable nucleic acid hybridization probes, Nat. Methods 12 (2015) 1191–1196.
[25] P.M. Bossuyt, J.B. Reitsma, D.E. Bruns, C.A. Gatsonis, P.P. Glasziou, L.M. Irwig, J. G. Lijmer, D. Moher, D. Rennie, H.C. De Vet, Towards complete and accurate reporting of studies of diagnostic accuracy: the STARD initiative, Radiology 226 (2003) 24–28.